INTERNATIONAL JOURNAL FOR NUMERICAL METHODS IN FLUIDS
Int. J. Numer. Meth. Fluids 2004; **45**:179–196 (DOI: 10.1002/fld.642)

Mesh adaptation as a tool for certified computational aerodynamics

E. Schall[1,†], D. Leservoisier[2], A. Dervieux[3,*,‡] and B. Koobus[4]

[1]*IUT Génie Thermique et Energie 1, Avenue de l'Université, 64 000 PAU, France*
[2]*SNECMA-Villaroche and INRIA, France*
[3]*INRIA Sophia-Antipolis, BP 92, 06902 Sophia Antipolis Cedex, France*
[4]*Université Montpellier II, CC. 051, 34095 Montpellier Cedex 5, France*

SUMMARY

Mesh convergence order is a key for certification of the accuracy of numerical solutions. A few available results and tools in mesh adaption are synthetized in order to specify a mesh converging method for adaptive calculation of compressible flows including shocks or viscous layers. The main design property for this method is early second-order convergence, where early means that the second-order convergence is obtained with coarse meshes. Copyright © 2004 John Wiley & Sons, Ltd.

KEY WORDS: computational fluid dynamics; mesh convergence; mesh adaptation

1. INTRODUCTION

While numerical methods and computers show impressive improvements, the numerical quality of CFD computations remains a delicate problem, see for example [1]. In particular, estimating approximation errors is one of today's more important challenges in CFD. Error estimates are progessively more pertinent for this issue (see References [2–4]), but mesh convergence is still the most popular tool. Mesh convergence theory and methods date back at least to Romberg [5]. They have been well studied, but in current compressible CFD, mesh convergence studies are still rather disappointing.

The fundamental assumptions of the theory are: (1) uniform order of convergence, (2) Cartesian or uniform meshes and (3) embedded meshes.

The uniform order assumption is, for example, the basis of the grid convergence index proposed in Reference [6]. Now a particular property of compressible flows is that they involve either strong singularities, such as shocks, or, in the viscous case, strong local gradients (viscous shocks, boundary layers). Thus the uniform order is in conflict with the computation of these singularities. Uniform refinements and modern shock capturing schemes will produce

*Correspondence to: A. Dervieux, INRIA Sophia-Antipolis, BP 92, 06902 Sophia Antipolis Cedex, France.
†E-mail: eric.schall@univ-pau.fr
‡E-mail: alain.dervieux@inria.fr

Received 26 November 2002
Revised 30 June 2003

various orders of convergence, a difficulty that is addressed in Reference [7] for inviscid flows with detached shocks. In the case of viscous flows, numerical order can be even more intricate since on very fine meshes, the numerical convergence will finally switch from first order to second order in shock region. In general, global second-order mesh convergence seems to be unattainable in most practical applications.

Let us analyse in greater detail both cases.

For the *case of genuine discontinuities*, thousands of papers were devoted during decades to design second-order accurate schemes for the Euler model that are able to compute accurately shocks. However, even a high resolution scheme is unable to converge at second order towards a discontinuous solution when it is combined with a uniform mesh refinement process, see for example [8]. This failure is related to the impossibility in interpolating accurately a discontinuous solution on a sequence of uniformly divided meshes. In a recent paper [9], the poor performance of P_1 interpolation of discontinuous functions in uniform mesh refinement was again put in evidence. Convergence order in L^2 norm is less than one. It was shown that, conversely, *adequate sequences of adapted meshes* can offer a higher order of convergence. But, in two or three dimensions, only the anisotropic mesh adaptation has the potential to produce a second-order convergence. Conversely, in Reference [10], we analyse for interpolation problems why and in which conditions anisotropic adaptation can be able to produce second-order accuracy on discontinuities.

In contrast, in the *case of viscous shocks*, it is true that second-order convergence should be always obtained when uniform refinement involves fine enough meshes. But, in practical cases, we generally do not observe the second-order convergence. This demonstrates that the usual asymptotical theory does not explain today's experience and should be extended.

Our study will rely on the following explanation: the 'viscous discontinuities' should be understood as behaving in some case as pure discontinuities, and in some case as smooth regions. Indeed, when the mesh which is used is not fine enough to capture the smooth thickness of the shock, then the viscous shocked flow calculations generally show a convergence order which is not better than the inviscid one, that is with a numerical order close to one.

The key goal of this work is then to identify an algorithm that will show *early second-order convergence* of viscous flows with discontinuities. And the key principle is to use a mesh adaptive method that is able to produce second-order accuracy on genuine discontinuities.

For doing this, we do not need to reinvent all the ingredients of the method. Instead, we shall use some well established ones (some of them are even available on the WEB), resulting from the recent mesh adaption studies. Mesh adaptation studies represent today an enormous amount of work. They involve many application studies in which meshes are improved in order to better compute some particular physics. They also involve theoretical developments dedicated to the better specification of a mesh adapted to a precise computation. A particular interesting emerging subject is the mathematical building of methods taking into account the whole process from a numerical scheme, local errors, and particularly *mesh specifications*. We refer for example to [2, 3]. Since an adapted mesh can be specified, this may mean that the mesh satisfying some specifications is somewhat unique in a class of equivalent meshes. Several teams have adopted this line of reasoning, see for example [11, 12].

After being specified, the adapted mesh must be built. This can be done by taking benefit from the recent progress in the elaboration of anisotropic meshes, either by a powerful improvement of the current mesh [11] or by its regeneration [12] according to the given metrics. The present work will use the latter option, although we believe the former is also

adequate. Of course, the flow resolution kernel has also to satisfy some accuracy properties on a wide class of meshes. We shall work with a well validated upwind finite-volume scheme of vertex-centred type.

The main contribution of this paper is to propose a combination of these methods that first will produce adapted solutions for a *fixed number of nodes*, and second will lead to *early second-order mesh convergence*. This will allow for a Romberg-type numerical quality analysis: once the second-order numerical order is *certified* we derive classically an estimate of the approximation error.

In the next section, we present the complete algorithm built with the above ingredients and designed for converging to the continuous solution. In Section 4, we compare the adapted mesh convergence with the classical uniform mesh convergence for academic test cases. Section 5 presents a case inspired by an industrial problem. Two other examples are presented in Section 6.

The plan is then as follows:

1. A mesh convergence algorithm
2. An academic test case
3. A more practical example
4. Turbulent flows
5. Conclusion

2. A MESH CONVERGENCE ALGORITHM

The purpose of the mesh convergence algorithm is to build an idea of the continuous solution to the flow problem by proposing:

– several approximate solutions and
– a rather reliable estimate on the accuracy of the solutions.

This will be obtained by an algorithm producing a set of solutions showing convergence to the continuous limit with an uniform order. This algorithm will involve a flow kernel, an adaptative mesh generator, and tools for comparing the solutions and certifying the convergence.

2.1. Flow kernel

Since we want to get second-order convergence to the continuous solution with sequences of adapted very irregular meshes, it is compulsory to have a numerical approximation that will be actually second-order accurate in these conditions. The spatial discretization scheme that we use is often referred to as a mixed finite element/finite volume scheme. It is based on a vertex-centred finite-volume method, with degrees of freedom located at triangle vertices and dual cells limited by triangle medians. It is combined with a P_1-Galerkin finite-element integration of the diffusive terms. For the stabilization of the advective terms, the scheme involves a MUSCL-type second-order Godunov-type upwinding built from the Roe Flux Difference Splitting with or without low Mach number correction. We refer to [13] for a description of the scheme and to [14] for analyses showing *second-order accuracy* on simplified models but rather arbitrary meshes, i.e. meshes that may involve very high local variation of mesh size,

but that are not too stretched. This accuracy order is the best (for this scheme) that can be observed on arbitrary flows, and in particular, the scheme does not enjoy superconvergence on Cartesian meshes [14]. This property is interesting for an accurate evaluation of convergence order.

2.2. Mesh adaptation with a fixed number of nodes

For a given number of nodes, we want to specify an adapted mesh. We seek a mesh adaption method which satifies the following properties:

(i) For a given mesh size, the method specifies essentially only one mesh and one discrete solution. By essentially, we mean that two meshes that produce in all region of computational domain about the same quality of approximation are just two representants of the same class of equivalence of meshes.
(ii) For a regular enough continuous solution, mesh description should be independant of mesh size. This will play the role of the embedded mesh assumption.
(iii) For singular solutions the mesh should enjoy second-order discontinuity capturing.

From the approximate flow solution we extract a particular scalar quantity defined at every vertex on the mesh, the *sensor*. To fix the idea, we take the Mach number. We do not think that the Mach number makes the best sensor. Its replacement by a better option would deserve a study that is beyond the scope of the present work. This point will be further discussed in the conclusion of this paper.

From an approximate Hessian matrix of the sensor we derive, as in Reference [12], the *metrics* (a 2×2 matrix defined also over the mesh). Two options are studied: (i) in the isotropic case, the matrix is the product of the identity matrix by a scalar taken equal to the absolute value of the largest eigenvalue of the above Hessian. (ii) in the anisotropic case, the matrix is essentially the absolute value of the Hessian, as proposed in Reference [12].

With the above rules of thumb (i) and (ii), it is possible to imagine a set of approximation method that would permit the metrics to converge to a smooth continuous one, which would have two consequences:

(1) In the case where the mesh size is specified, the continuous metric would be unique, and in the smooth case, and then the problem is well posed (flow is well posed, metric is a passive variable, function of flow). This is a good option if we want to have also a unique discrete solution.
(2) When the above solution is obtained for a sequence of mesh size tending to an infinite number of nodes, then, in both adaptive and uniform options, couples (flow, normalized metric) converge to a unique continuous analog (continuous flow, continuous metric).

These properties have not been proven but have been observed on practical examples. It remains to consider (iii), i.e. discontinuity second-order capturing capacities. As mentioned in the introduction, we adopt the standpoint explained in Reference [10]. In this paper, the authors observe that only a part of adaptive methods are able to capture genuine discontinuites with second-order accuracy, and identify (a) second derivative based sensors and (b) anisotropic adaptation as particular features favourizing second-order discontinuity capturing.

Once the metrics are obtained, they are used as input in a *mesh regenerator*, for rebuilding a new mesh following the metrics and involving approximatively the prescribed number of

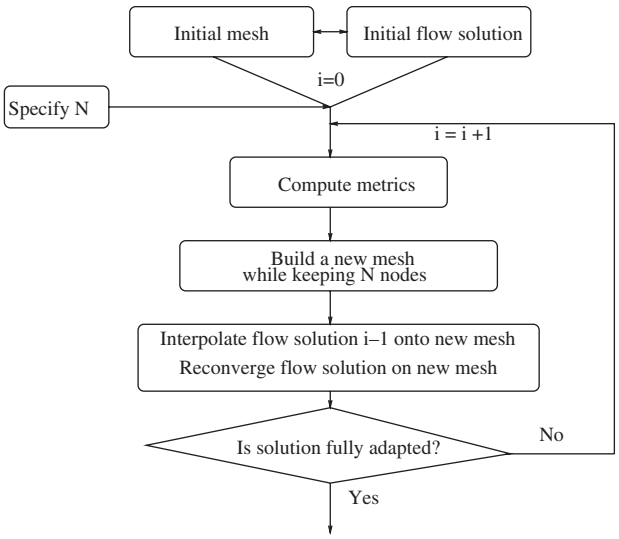

Figure 1. Adaptative interpolation. This loop provides a couple (mesh, flow solution) for a prescribed number of nodes N.

vertices. For this task, we have applied an existing software, BAMG, proposed by Hecht and co-workers, see Reference [12]. BAMG uses the metrics defined on the initial mesh in order to test if some local improvement is necessary. Different local tools, such as edge suppression and swapping, vertex suppression, addition, and reallocation are applied until the metrics are satisfied, i.e. typically, every edge has a length close to unity for the considered metrics.

A crucial issue is the iteration and *non-linear convergence of adaptation* fixed point. In order to obtain the more or less unique mesh that is perfectly adapted according to our algorithm, the new adapted mesh is re-injected in an adaptation loop in order to get a new solution, then a new mesh, again with the same prescribed number of nodes. This algorithm is sketched in Figure 1. Typically, after 6 to 10 cycles, the mesh and the solution do not change significantly and *the adaptation loop is declared as iteratively converged.*

An accurate interpolation is applied to transfer solutions between the successive meshes in order to save computational effort. This tool is described in the sequel.

The result of this process is to construct an approximate adapted solution for a prescribed number of nodes.

2.3. Mesh convergence, transfers of solutions and numerical convergence order

2.3.1. Mesh convergence sequence. We propose to compute the numerical order from three approximate solutions for three prescribed different numbers of vertices: N, $4N$, $16N$. We note that in the case of adapted meshes, the meshes are not embedded. Further, the ratio between the vertices of two meshes does not need to be chosen as a multiple of 4. The choice of this ratio has just the advantage of an easy comparison with a classical embedded mesh convergence (uniform mesh division).

2.3.2. Transfers to a unique mesh. In order to compare solutions and to be able to compute their differences, we project all solutions on the finest mesh of the considered series.

Two types of projection were tried and compared. The P_1 projector will keep exactly the P_1 interpolation of the coarse mesh after transfer to any finer mesh. Beside this canonical option, and in order to have a transfer more robust in case of non-embedded meshes, we have also applied a projector which interpolates the function with a P_2 operator inside triangles (P_3 along edges) built from the knowledge of average gradients at vertices. We shall refer to it as the P_2 projector.

2.3.3. Evaluation of the numerical order of convergence. The convergence assumption is set for the L^2 space, by analogy with the elliptic finite-element theory, but with an estimate of the remainder:

$$u_h = u + N^{-1}u^1 + N^{-3/2}O_{L^2}(1) \tag{1}$$

where $O_{L^2}(1)$ is a function which is bounded in L^2 norm when N tends to infinity.

Let M_1, M_2, M_3 be a triplet of meshes with a ratio of vertex numbers equal to four and U_1, U_2, U_3 the corresponding solutions.

We can compute the ratio q between the two consecutive deviations in L^2,

$$q = \frac{\|U_1 - U_2\|_{L^2}}{\|U_2 - U_3\|_{L^2}}$$

The convergence order is evaluated by solving $\alpha = \ln q / \ln 2$. In practice, we shall say that the second-order convergence is observed when the numerical order lies between 1.6 and 2.2:

$$\alpha \in [1.6, 2.2] \tag{2}$$

2.3.4. Global algorithm. It writes:

0. *Start with two adapted solutions* $\mathscr{S}_N$ *and* $\mathscr{S}_{4N}$ *with* N *and* $4N$ *nodes.*
1. *Compute an adapted solution* $\mathscr{S}_{16N}$ *with* $16N$ *nodes.*
For this, iterate Algorithm 1 *until convergence.*
2. *Transfer all solutions to the finest mesh. Test whether the triplet of* $\mathscr{S}_N$, $\mathscr{S}_{4N}$, $\mathscr{S}_{16N}$ *satisfies the numerical order statement* (2).
3. *If not, set* $N = 4N$ *and go to* 1.
4. *If yes, stop.*

3. AN ACADEMIC TEST CASE

Obtaining a second-order convergence on three meshes with the above ratio $(N, 4N, 16N)$ is a difficult task, even for very simple and smooth flows such as 2D airfoil flows at a very low Reynolds, Rey = 73. The airfoil geometry is the standard NACA0012, and two farfield Mach numbers are considered, $M = 0.85$ and 1.2.

3.1. Uniform refinement study

A traditional mesh convergence study relies on a series of *embedded* meshes. It is the occasion to check how mesh convergence works with *unstructured* meshes. In order to have four

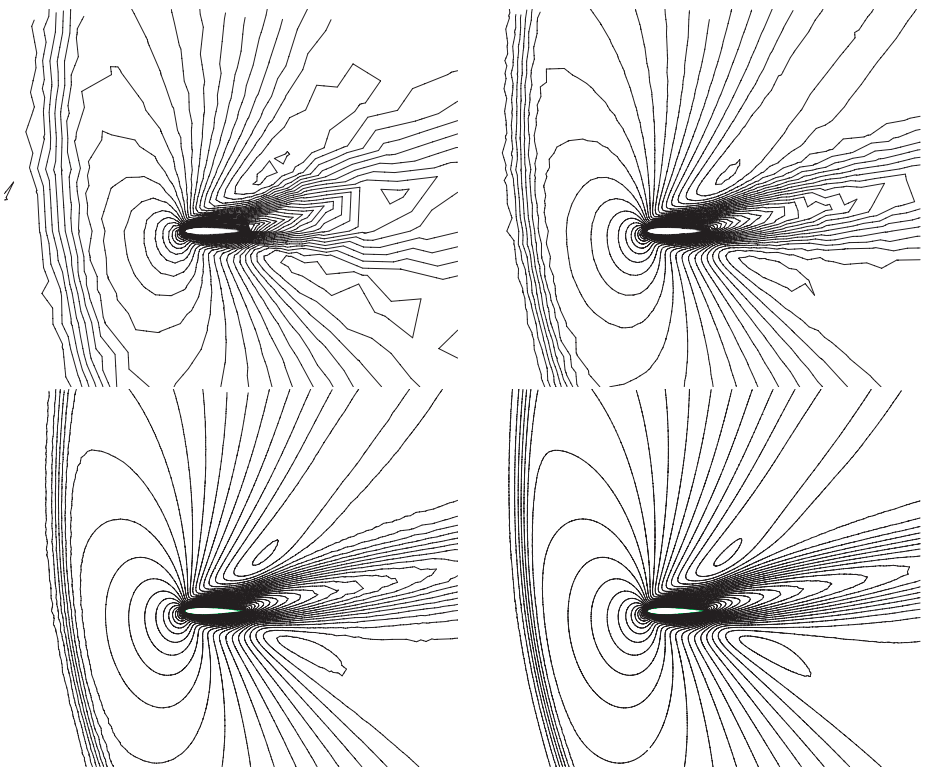

Figure 2. Uniform refinement: pressure contours for the supersonic flow case with embedded meshes of respectively (from left to right and top to bottom) 800, 3114, 12 284 and 48 792 vertices.

meshes that are at the same time embedded and unstructured, we start from a fully unstructured coarse mesh and then the first intermediate mesh is obtained by dividing each triangle into four equal subtriangles. The third mesh is derived from the first intermediate one by dividing again each triangle in four equal triangles. The last (finest) mesh is in turn obtained by division of the previous one. The number of vertices (=nodes) of these meshes are, respectiveley, $800, 3114, 12\,284, 48\,792$. By the way, we note that the new meshes are still unstructured, but they have lost the smoothness of the local mesh size, since this mesh size stays constant over macro-triangles and varies abruptly at the limits of the macro-triangles (the second-order derivative of the local mesh size is zero over macro-triangles, but is a Dirac at their limits). In the case of an elliptic finite-element study, this loss of regularity would not be an obstacle to second-order convergence and we assume this property extends to our case. For each computation, the equation residual is converged down to the zero machine. Figure 2 gives an idea of the quality of the various computations. We observe on the coarsest results some oscillations that indicate that the mesh is too coarse and irregular. We consider two sequences of three meshes:

(a) meshes with $(800, 3114, 12\,284)$ nodes, denoted by mesh sequence (a),
(b) meshes with $(3114, 12\,284, 48\,792)$ nodes, denoted by mesh sequence (b).

Table I. Uniform refinement: several measures of L^2 convergence order when two types of interpolation towards the finest mesh are used. Sequence (a) involves meshes with $(800, 3114, 12\,284)$ nodes, sequence (b) involves meshes with $(3114, 12\,284, 48\,792)$ nodes.

1 Variables	Mach 0.8 (P1) sequence (a)	Mach 0.8 (P1) sequence (b)	Mach 0.8 (P2) sequence (a)	Mach 0.8 (P2) sequence (b)
Rho	1.023	1.883	1.124	1.984
Rho*U	0.768	1.617	0.889	1.793
Rho*V	0.701	1.612	0.780	1.716
2 Variables	Mach 1.2 (P1) sequence (a)	Mach 1.2 (P1) sequence (b)	Mach 1.2 (P2) sequence (a)	Mach 1.2 (P2) sequence (b)
Rho	0.873	0.977	0.948	1.139
Rho*U	0.905	1.645	1.016	1.851
Rho*V	0.993	0.970	1.024	1.121

We present in Table I the numerical convergence orders evaluated as explained in Section 2. We restrict our study to the three first unknowns of the Navier–Stokes equations, density and momentums. We observe first that computing the order of convergence from P_2 interpolations onto the finest mesh show an improvement in the numerical convergence order of about 5–10%. We shall consider in the sequel only this P_2 interpolation post treatment. All the convergence studies on the sequence of coarsest meshes (a) produce a convergence order around 1. This means that not all of the three calculations are in the asymptotic region where dividing the mesh step by two ensures a four times smaller error. Convergence orders for the subsonic case with the finest meshes (b) appear to be near 2. For the supersonic case, convergence order is near 1, even with the sequence of finest meshes (except for the horizontal velocity where we get the second order). We attribute this difference to the influence of the bow shock, which is not well captured on the different meshes. To sum up, the second-order accuracy of the approximation scheme on unstructured meshes is confirmed, but the above sequence of meshes shows that only fine meshes give some access to second-order accuracy and this, only for solutions without viscous shock.

3.2. Isotropic adaptation study

Now the computations are done only by the mesh adaptation process described in Section 2. A unique sensor, the Mach number is used, and the maximum eigenvalue of its local Hessian is used as an isotropic metric. The iteration between computation and mesh regeneration applied until convergence is fully obtained between mesh and solution (typically 10 times).

We observe that with the sequence of finest meshes, a second-order convergence is reached for the two farfield Mach numbers. We recall that from one case to the other one, two adapted meshes with an equivalent fineness level are different since they are adapted to different flows. Second-order convergence is not observed with the coarse sequences, except for the horizontal momentum (Table II).

Table II. Isotropic adaptative refinement: several measures of L^2 convergence order.

Variables	Mach 0.8 sequence (a)	Mach 0.8 sequence (b)	Mach 1.2 sequence (a)	Mach 1.2 sequence (b)
Rho	1.05	1.78	1.00	2.13
Rho*U	1.87	1.89	1.61	1.55
Rho*V	1.26	1.71	0.99	1.80

Table III. Anisotropic adaptative refinement: several measures of L^2 convergence order.

Variables	Mach 0.8 sequence (a)	Mach 0.8 sequence (b)	Mach 1.2 sequence (a)	Mach 1.2 sequence (b)
Rho	1.74	2.01	1.62	2.15
Rho*U	1.58	2.08	1.78	1.75
Rho*V	1.83	1.66	1.85	1.87

3.3. *Anisotropic adaptation study*

The absolute value of the local Mach number Hessian is used as an anisotropic metric. From Table III, we deduce that, with the anisotropic refinement, second-order convergence is obtained even with the coarse sequences of refinement, for both cases, subsonic and supersonic, and for the three considered variables. This convergence is obtained with meshes involving a number of vertices that is four times smaller than with the previous strategies. This ratio depends on the Reynolds number and would be much larger for thinner shocks.

Remark

As mentioned earlier, we have not considered the total energy convergence, and in fact, with the Mach number as adaptative sensor, we do not get for the energy a convergence as good as for the three other flow variables. As a result, the proposed calculations are not adequate for the evaluation of lift and drag coefficients, as they depend on the total energy.

3.4. *Error level*

The validation of second-order accuracy, that is the maximal theoretical order of accuracy, allows to derive an error estimate of the L^2 error for the finest mesh among the coarse sequences.

Let us denote by u_2 the solution computed with the adapted anisotropic mesh of 3114 vertices and u_3 the solution computed with the adapted anisotropic mesh of 11 938 vertices for the supersonic case.

Since we have second-order convergence, and starting from the deviation:

$$||u_2 - u_3||_{L^2} = 1.802 \times 10^{-4}$$

we derive the following *error estimate*:

$$||u_3 - u||_{L^2} \leqslant (1.802/3)\ 10^{-4} = 0.600 \times 10^{-4} \tag{3}$$

As can be expected, this estimate is coherent with the calculation of u_4 done with the finest adapted anisotropic mesh. Indeed, we have:

$$||u_3 - u_4||_{L^2} = 5.637 \times 10^{-5}$$

which confirms the accuracy of (3).

We observe that the error estimate for u_4 would be of 2×10^{-5}, a rather small error for a second-order accurate computation.

As a conclusion, this analysis gives some insurance that second-order convergence is reached, 'certified', and that the approximation error is reasonably well predicted by the convergence model.

4. A MORE PRACTICAL EXAMPLE

Turbo-engines combustion chambers are limited by metallic walls with a large number of small perforations. These perforations allow an external colder fluid to enter into the combustion chamber and to facilitate a colder boundary layer to protect the wall against extreme heat. The way only one hole interfers with internal and external flows is difficult to compute. Indeed the flow is a low Mach number flow (Mach number is about a few thousandths), but asymptotic models should not be used since the size of fluctuations of pressure, density and temperature are forced to non-small values by farfield external and internal flow prescription. See Reference [15] for a discussion about this modelization issue and for the low Mach number correction applied to the approximation. Another important difficulty which we shall not address in the present study is the size of the hole, that is smaller than the turbulent boundary layer thickness and induces important local laminar behaviours. In the present study, we restrict to a laminar 2D model.

The same numerical scheme as in the previous sections is applied, except that the Turkel preconditioner is introduced inside the stabilization term of the Roe flux difference splitting. The accuracy of the resulting preconditioned scheme is discussed in Reference [15]. We first give in Figure 3 a rough idea of the flow: the upper boundary layer disappears at hole location due to suction, the lower boundary layer is not much affected. The boundary conditions specify some uniform pressure levels at farfield, with two different values, at upper part and at lower part of the geometry. The velocities are on each part set equal at farfield. The wall condition is an isothermal one, with the same prescribed temperature for both sides of the wall. The Reynolds number with respect to the perforation section is 5000. Experimental results are not yet available.

In order to compute a 'certified solution', we apply the proposed method, with mesh sizes of about 3000, 12 000, 48 000 vertices. In order not to be handicaped by possible algorithm convergence problems, the study uses the isotropic mesh adaptation procedure. This is possible due to the fact that the main singularities are located at geometry angles. After adaptation, the final meshes involve respectively 2963 vertices for Mesh 1, 11 864 for Mesh 2, and 47 451 for Mesh 3. We observe, see for example Figure 4 for the coarsest mesh, that the boundary layer in the perforation needs a significantly stronger local refinement than the plate boundary layers. The mesh convergence of the flow is rather good between the coarse mesh and the fine one, as illustrated by the Mach number and pressure contours depicted respectively in Figures 5 and 6. All the results are transferred to the finest mesh by using

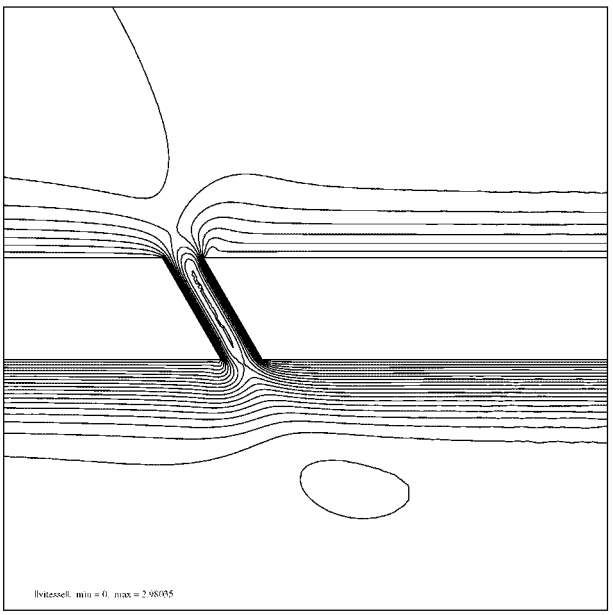

Figure 3. Low Mach flow near a perforated wall: contours of the velocity modulus, from 0 to 3 m/s. External flow is on upper side, with a smaller mean velocity, and a higher pressure; both flows go from left to right. Mean temperatures of the two flows are identical.

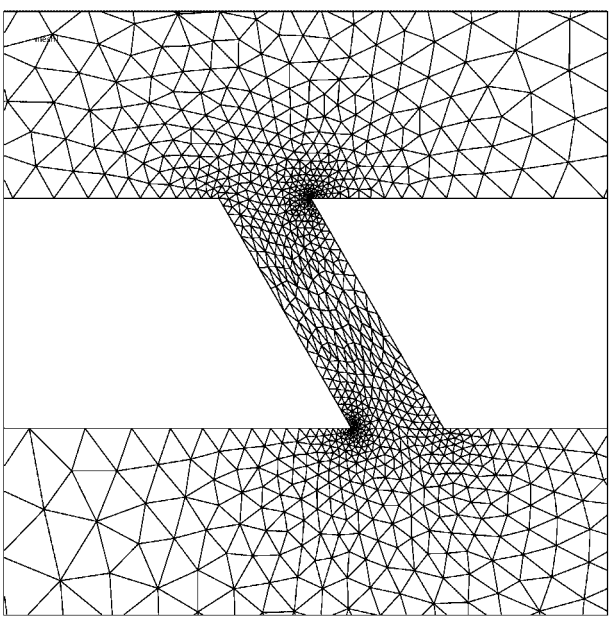

Figure 4. Flow in a perforated wall: zoom of the coarsest adapted mesh (3000 nodes).

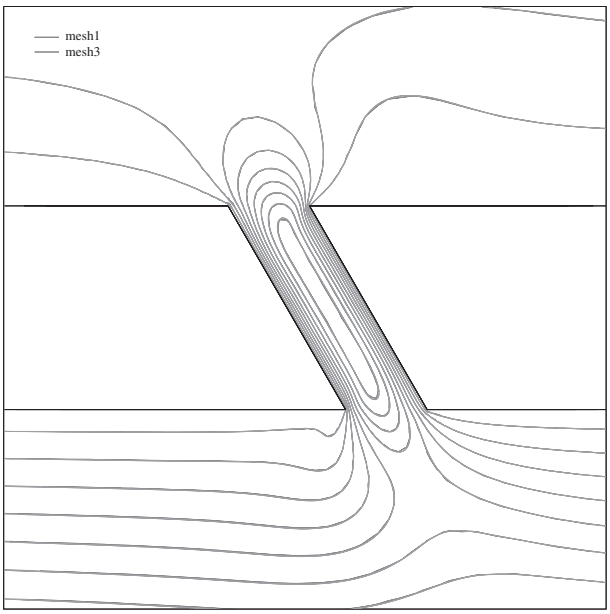

Figure 5. Flow in a perforated wall: Mach contours comparison, solutions computed with meshes 1 (coarsest) and 3 (finest).

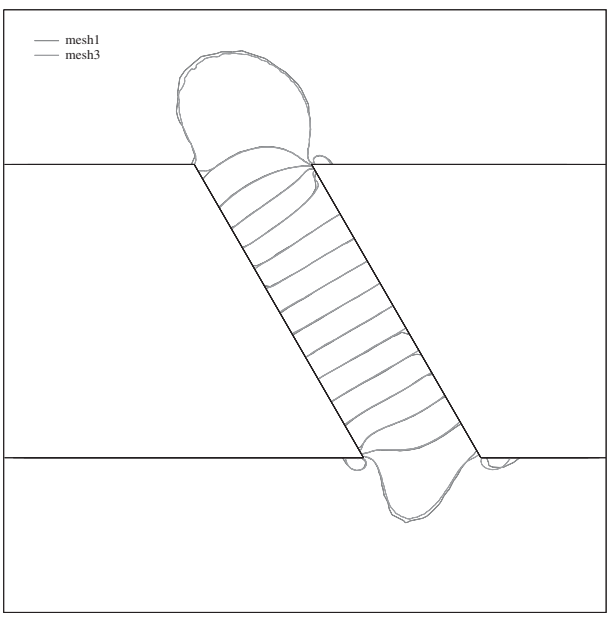

Figure 6. Flow in a perforated wall: pressure contours comparison, solutions computed with meshes 1 (coarsest) and 3 (finest).

Table IV. Isotropic adaptative refinement for the perforated wall computation: numerical order of convergence for the four dependant variables.

Variables	$\|\|U1-U2\|\|$	$\|\|U2-U3\|\|$	Numerical order
Rho	0.00408	0.00101	2.01
Rho*U	2.90405	0.41886	2.79
Rho*V	1.33931	0.25401	2.39
Rho*E	235.002	614.916	1.38

quadratic interpolation. Then, the numerical convergence rate (Table IV) is close to second order, except for the total energy. The L^2 error for the density on Mesh 3, for example, is estimated as less than 3×10^{-4}.

5. TURBULENT FLOWS

The proposed method has been applied to turbulent flows computed with a statistical model. The standard $k-\varepsilon$ model with a logarithmic wall law was applied. In order to allow for a mesh convergence, it is essential that the thickness of the analytic wall region is prescribed at the same value for the different meshes (and does not vary with the mesh size). Except the turbulence equations, the same numerical scheme as in Section 3 is used. In practice, turbulent statistical models are used for obtaining rather global informations. This does not mean that the task is easier. Friction coefficients for example are difficult to evaluate because in general the numerical scheme does not exhibit a sufficiently strong convergence property for providing an accurate derivative at the boundaries. This is often compensated by superconvergence properties as those arising when the mesh is kept cartesian. *A priori*, we cannot get this advantage in our mesh adaptation strategy. In a first calculation we consider the supersonic flow at the leading edge of a flat plate (without angle of attack). The inflow Mach number is 1.76 and the Reynolds number is 5.4×10^5. For flat elements, the approximation is adapted according to Reference [16].

We try to evaluate accurately the value of the friction coefficient $C_f(P)$ computed from the vertical derivative of the horizontal velocity component

$$C_f = \mu \left.\frac{\partial u}{\partial y}\right|_{\text{Wall}}$$

at a fixed point P located 1 m down stream of the leading edge. Convergence of this scalar output is measured by difference with a reference anisotropic adaptative calculation involving 30 000 vertices. The Mach number is chosen as sensor for adaptation. In the two typical meshes presented in Figure 7, the features of this rather elementary flow are easily recognized. In Figure 8, we illustrate that, although not very regular, the mesh convergence of $C_f(P)$ is clearly of second order when the proposed mesh adaptative method is applied in its anisotropic version. It is obtained with meshes not larger than 3000 nodes. With 4000 nodes the relative error is about 2%, and about 0.3% for 20 000 vertices. In the case of the isotropic adaptation, the second-order convergence is obtained only with meshes larger than 15 000 nodes.

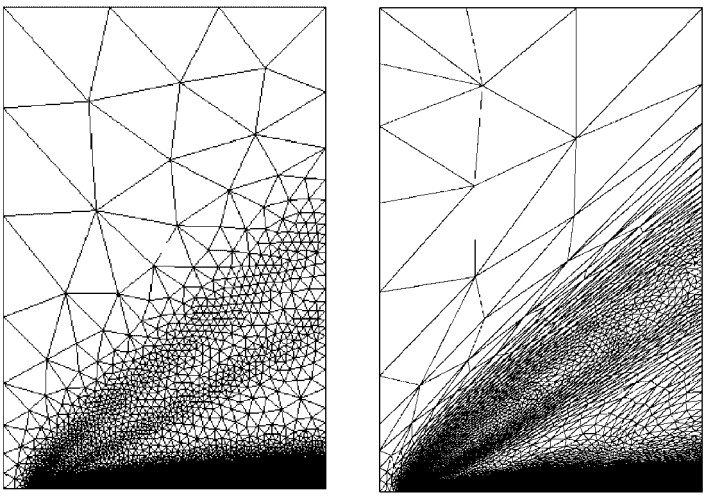

Figure 7. Two typical adapted meshes, isotropic (left) and anisotropic (right), for the supersonic flat plate calculation.

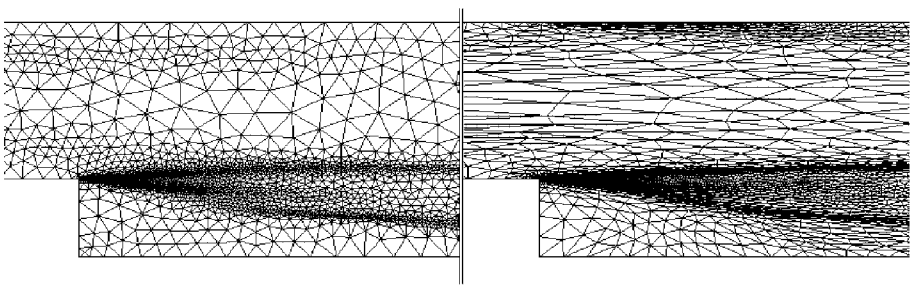

Figure 8. Two typical adapted meshes, isotropic (left) and anisotropic (right), for the back step flow calculation, with this size of mesh, and due to the wall law, the wall boundary layers are not yet refined.

In a second calculation, the classical flow over a backward facing step is computed [17, 18]. In Reference [19], non-monotonic convergence is observed for this rather difficult test case. The same compressible turbulent model is applied with a Mach number of 0.1. The scalar output under investigation is the abscissa of the reattachment point. The reference calculation is obtained with the anisotropic adaptation and 35 000 vertices. The velocity modulus is the sensor. For this mesh, a reattachment abscissa of 6.66 is obtained, an unusual and surprisingly good value for a wall law model. We have compared the isotropic and anisotropic adaptative strategies, see Figure 9. Mesh convergence of reattachment abscissa is obtained with second-order accuracy when the proposed anisotropic method is used with meshes involving 1000 vertices, see Figure 10. On the contrary, the isotropic investigation still produced a poor convergence rate close to unity, with meshes of 10 000 vertices, see Figure 11.

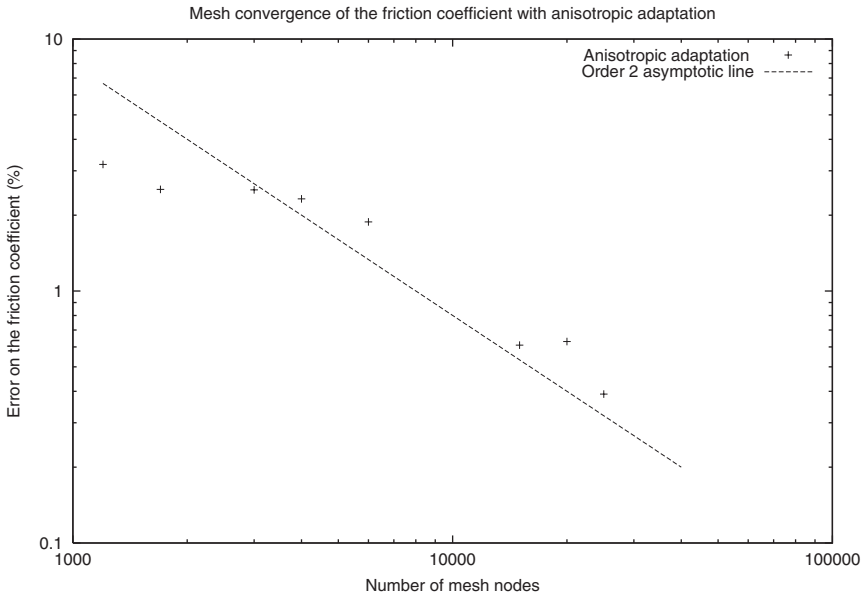

Figure 9. Flat plate flow calculation with anisotropic adaptation: mesh convergence of friction velocity (straight line indicates second-order accuracy). In abscissa we have the number of nodes and in ordinate the friction velocity error.

6. CONCLUSION

A method for second-order numerical convergence relying on mesh adaption has been proposed. It uses two important ideas:

- mesh adaption has to be governed by metrics that may converge to a continuous one. This is allowed by a continuous based definition of the metrics and a non-linear adaption convergence.
- early discontinuity capturing methods are the key for practical applications. They can be defined as capturing genuine discontinuities at second order.

We have proposed a set of tools for obtaining what we call 'a certified numerical simulation'. Starting from an approximation enjoying a good behaviour on irregular meshes, we have combined it with an adaptation loop. An important point is that mesh adaptation is always performed for a fixed number of nodes. The third subset of tools deals with the transfers of solutions between meshes and the solutions comparison for the certification of the convergence rate to the continuous limit.

The first examples of application of our mesh convergence algorithm are two classical airfoil flows. We have shown that second-order convergence with uniform refinement is not easily obtained even with a rather large number of nodes, while, with the proposed anisotropic mesh adaptation approach, second-order convergence is observed with a much smaller number of nodes. We have shown that the proposed method applies successfully to several other CFD

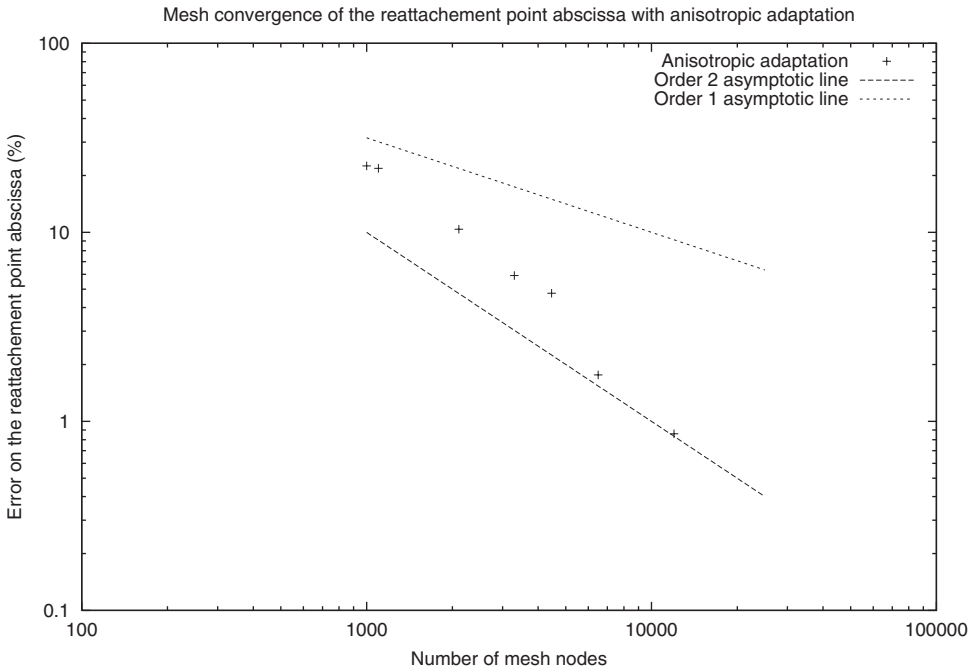

Figure 10. Back step calculation with anisotropic adaptation: mesh convergence of the reattachment point abscissa.

calculations. In the case of high Reynolds turbulent flows, the uniform refinement does not produce any reasonable result. The isotropic option is clearly inaccurate.

Although less rigorous than an exact *a posteriori* error estimate, the proposed mesh convergence analysis is a rather reliable method and carries some security in the use of the computed results.

The cost of our computational method is not very high, since the coarse adapted meshes produce already rather accurate solutions, and we can start with medium coarse mesh the solutions as initial conditions on finer mesh.

Of course this work shows the need of several extensions.

On a theoretical standpoint, we think it is necessary to complete our work by proposing a better metric definition for mesh adaptation to the solution of a Partial Differential Equation. Indeed, choosing just, as we did, a clever sensor (like Mach number) is an option which lacks a firm theoretical basis. In computations, this option appeared to be not adequate for total energy and pressure convergence. Error models relying on the new methods of adjoint states for mesh adaptation are under study [20].

We did not solve here the case of high Reynolds flows computed 'up to the wall'. This context carries particular difficulties that merit a focused investigation. The extension to unsteady calculations is also a difficult issue since many related problems are not well solved (in particular the definition of accurate and conservative transfers between two meshes).

Concerning a routine and transparent practical use of the proposed method, we think it today possible in 2D since we could easily automate the present algorithm thanks to the

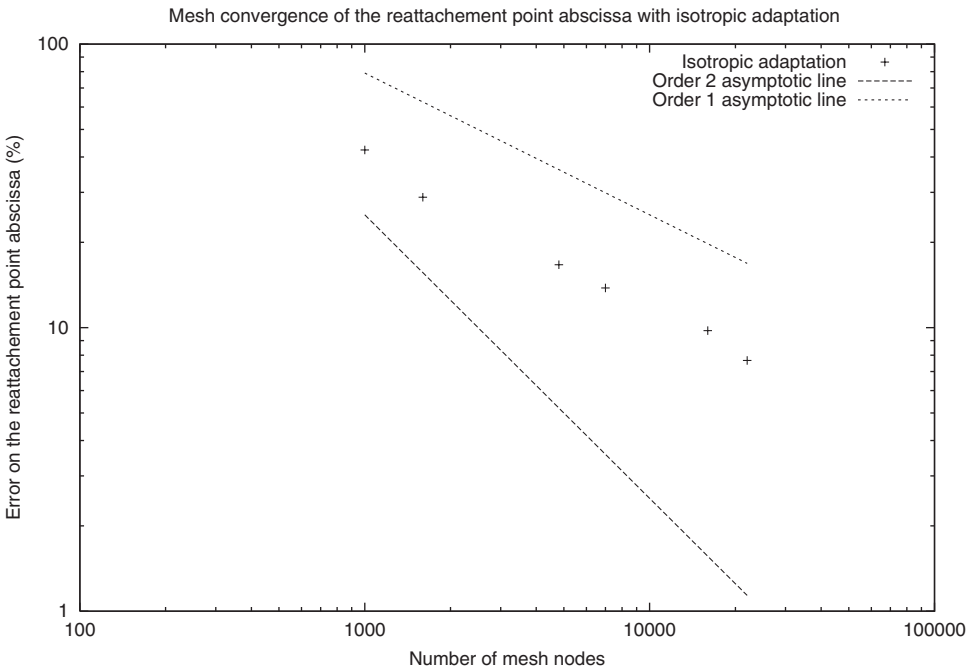

Figure 11. Back step calculation with isotropic adaptation: mesh convergence of the reattachment point abscissa.

robustness of all its components. A remeshing loop is much more easy to handle in 2D than in 3D. In particular, boundary definition in 2D is not as complex as in 3D. But we think that progresses in 3D CAD and mesh generation methods are fast enough to allow transparent 3D mesh adaptation in a very few years.

ACKNOWLEDGEMENTS

We thank Stephen Wornom for kindly proof reading this paper.

REFERENCES

1. Hutton AG, Casey MV. Quality and trust in industrial CFD: a European initiative. *AIAA paper* 2001-0656, 2001.
2. Becker R, Braack M, Rannacher R. Numerical simulation of laminar flames at low mach number with adaptative finite elements. *Combustion Theory and Modelling* 1999; **3**:503–534.
3. Giles MB, Süli E. Adjoint methods for PDEs: *a posteriori* error analysis and postprocessing by duality. In *Acta Numerica* **11**. Cambridge University Press: Cambridge, 2002; 145–236.
4. Fortin M (ed.). Estimations a posteriori et adaptation de maillages (partly in French). Special issue of the *Revue Europeenne des Elements Finis* Hermes Science, Paris, France, 2000.
5. Romberg W. Vereinfachte numerische Integration Det Kongelige Norske Videnskabernes Selskabs Forhandlinger, Trondheim 1955; **28**:30–36.
6. Roache PJ. Perspectice: a method for uniform reporting of grid refinement studies. *Journal of Fluid Engineering* 1994; **116**(3):405–413.
7. Roy CJ. Grid convergence error analysis for mixed-order numerical schemes. *AIAA Journal* 2003; **41**:4.

8. Carpenter MH, Casper JH. Accuracy of shock capturing in two spatial dimensions. *AIAA Journal* 1999; **37**(9):1072–1079.
9. Coudière Y, Palmerio B, Dervieux A, Leservoisier D. Accuracy barriers in mesh adaptation. *INRIA Research Report* No. 4528, August 2002. http://www-sop.inria.fr/rapports/sophia/RR-4528.html.
10. Leservoisier D, George PL, Dervieux A. Métrique continue et optimisation de maillage. *INRIA Research Report*, RR-4172, April 2001 (in French).
11. Habashi WG, Dompierre J, Bourgault Y, Ait-Ali-Yahia D, Fortin M, Vallet M-G. Anisotropic mesh adaptation: towards user-independent, mesh-independent and solver-independent CFD solutions: Part I: general principles. *International Journal for Numerical Methods in Fluids* 2000; **32**:725–744.
12. Castro-Díaz MJ, Borouchaki H, George PL, Hecht F, Mohamadi B. Anisotropic adaptative mesh generation in two dimensions for CFD. *Numerical Methods in Engineering '96*; *Proceeding of the Second ECCOMAS Conference on Numerical Methods in Engineering*, Wiley: New York, 9–13 September 1996; 181–186.
13. Dervieux A. Steady Euler simulations using unstructured meshes, Von Karman Institute for Fluid Dynamics. *Lecture series 1985-04*, *Computational Fluid Dynamics*, 1985. And also Geymonat (ed.). *Partial Differential Equations of hyperbolic type and Applications*. World Scientific: Singapore, 1987.
14. Mer K. Variational analysis of a mixed element volume scheme with fourth-order viscosity on general triangulations. *Computer Methods in Applied Engineering* 1998; **153**:45–62.
15. Schall E, Viozat C, Koobus B, Dervieux A. Computation of low Mach number thermical flows with implicit upwind methods. *Journal of Heat and Mass Transfer* 2003; **46**:3909–3926.
16. Viozat C, Held C, Mer K, Dervieux A. On Vertex-centered unstructured finite-volume methods for stretched anisotropic triangulations. *Computer Methods in Applied Mechanics and Engineering* 2001; **190**(35–36): 4733–4766.
17. Kline SJ, Cantwell BJ, Lilley GM. *Proceedings of the 1980-81 AFOSR-HTTM Stanford Conference on Complex Turbulent flows*. Stanford University Press: Stanford, CA, 1981.
18. Kim J, Kline SJ, Johnston JP. Investigation of a reattaching turbulent shear layer: flow over a backward-facing step. *Journal of Fluid Engineering* 1980; **102**:302–308.
19. Celik J, Karatekin O. Numerical experiments on application of Richardson extrapolation: application to some simple turbulent flow calculations. *Journal of Fluid Engineering* 1997; **119**(3):584–590.
20. Courty F. *Optimisation Différentiable en Mécanique des Fluides Numérique*, Ph.D. thesis, Université Paris-Sud, 2003.

